

Squeezing via spontaneous rotational symmetry breaking in a four-wave mixing cavity

Ferran V. Garcia-Ferrer, Carlos Navarrete-Benlloch, Germán J. de Valcárcel and Eugenio Roldán

Abstract—We predict the generation of noncritically squeezed light through the spontaneous rotational symmetry breaking occurring in a Kerr cavity. The model considers a $\chi^{(3)}$ cavity that is pumped by two Gaussian beams of frequencies ω_1 and ω_2 . The cavity configuration is such that two signal modes of equal frequency $\omega_s = (\omega_1 + \omega_2)/2$ are generated, these signal fields being first order Laguerre–Gauss modes. In this system a spontaneous breaking of the rotational symmetry occurs as the signal field corresponds to a Hermite–Gauss TEM mode. This symmetry breaking leads to the perfect and non-critical (i.e., non dependent on the parameter values) squeezing of the angular momentum of the output TEM mode, which is another TEM mode spatially orthogonal to that in which bright emission occurs.

Index Terms—quantum fluctuations, four-wave mixing, nonlinear optics, squeezed light.

I. INTRODUCTION

Squeezed light is a kind of radiation exhibiting reduced fluctuations with respect to vacuum in some special observable. This occurs at the obvious expense of an increase in the fluctuations of its canonical pair, as followed by the Heisenberg uncertainty relation satisfied by the couple. In a single mode field these canonically related observables correspond to orthogonal field quadratures, which are equivalent to the position and momentum of a harmonic oscillator. Squeezing is a macroscopic manifestation of quantum phenomena that is attracting continuous attention since the late seventies of the past century [1], [2], [3]. Nowadays a renewed interest has arisen because of the importance of squeezing in generating continuous variable entanglement, which is a central issue for continuous variable quantum information purposes [4].

Squeezed light is generated by means of nonlinear optical processes, such as parametric down-conversion or four-wave mixing. The squeezing level attainable in such nonlinear optical processes depends on the interaction time that is limited by the nonlinear medium length. Thus in order to increase the squeezing level, these processes are usually confined to occur within an optical cavity. In this way the squeezing level can reach the largest possible levels at the system bifurcation

points such as, e.g., at the emission threshold. Squeezing levels as large as 90% (10dB reduction respect to vacuum fluctuations) have been recently reported [5], [6] in such conditions in degenerate optical parametric oscillators (DOPOs). However perfect squeezing (i.e., the complete suppression of quantum fluctuations in a field observable) cannot be achieved in these conditions because complete suppression of fluctuations in a mode quadrature implies the existence of infinite fluctuations in the other quadrature, what would require infinite energy in the process.

Nevertheless perfect squeezing could be actually produced and we have recently proposed a way for obtaining it [7]. The idea can be put in short as follows. Consider a nonlinear optical process in which two photons with equal frequency are generated, each photon corresponding to ± 1 orbital angular momentum (OAM) Laguerre–Gauss mode. This is equivalent to generating two photons in a TEM₁₀ Hermite–Gauss mode whose orientation in the transverse x-y plane is determined by the phase difference between the two Laguerre–Gauss photons, let us denote it by ϕ . Now assume that ϕ is not fixed as it occurs, e.g., in a down-conversion process. This amounts to saying that the orientation of the Hermite–Gauss mode is not fixed as ϕ is the angle formed by the Hermite–Gauss mode with respect to the x-axis. In these conditions we can expect the occurrence of arbitrarily large fluctuations in the Hermite–Gauss mode orientation, which suggests that the canonical pair of ϕ , namely the angular momentum $-i\partial/\partial\phi$, could be perfectly fixed. But the angular momentum of a TEM₁₀ mode forming an angle ϕ with respect to the x-axis is another TEM₁₀ mode forming an angle $\phi + \pi/2$ with respect to the x-axis. Then this mode could exhibit perfect squeezing in one of its field quadratures. Notice that the concept of bifurcation is not involved in this discussion and that the variable exhibiting arbitrary fluctuations is an angle. Then, a priori, perfect squeezing is possible in such a process as "infinite" fluctuations are possible in the fluctuations of ϕ .

In Refs. [7], [8] we have recently theoretically demonstrated the above ideas in a model of DOPO tuned to the first transverse family at the down-converted frequency. The requirement that the angle ϕ can take any possible value (i.e. that the phase difference between the two Laguerre–Gauss modes be arbitrary) is nothing but the requirement that the system be rotationally invariant around the optical cavity axis. Hence the resulting squeezing can be understood too as the result of the spontaneous breaking of this rotational symmetry, as the emitted Hermite–Gauss mode is obviously no more rotationally invariant. In [9] we extended this study to DOPOs having different transverse families resonating at the down-

All the authors are with Departament d'Òptica, Universitat de València, Dr. Moliner 50, 46100-Burjassot, Spain. (e-mail: carlos.navarrete@uv.es)

The authors want to thank Alberto Aparici for his help with the final L^AT_EX code.

This work has been supported by the Spanish Ministerio de Ciencia e Innovación and the European Union FEDER through Projects FIS2005-07931-C03-01 and FIS2008-06024-C03-01. C. Navarrete-Benlloch is grant holder of the Programa FPU del Ministerio de Ciencia e Innovación.

This work has been submitted to the IEEE for possible publication. Copyright may be transferred without notice, after which this version may no longer be accessible.

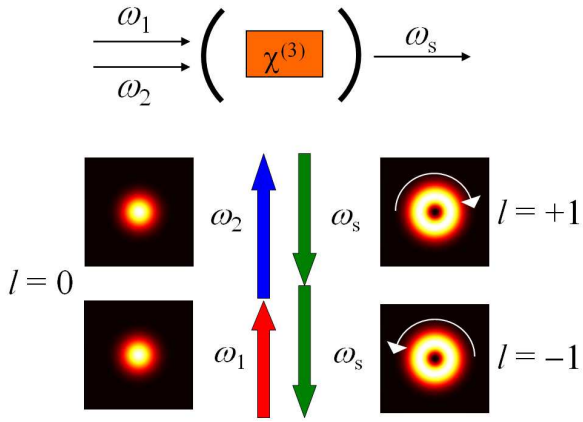


Figure 1.- Scheme of the system. A $\chi^{(3)}$ medium is confined within an optical cavity and pumped by two Gaussian beams of frequencies ω_1 and ω_2 . The cavity tuning is such that two signal modes with frequency $\omega_s = (\omega_1 + \omega_2)/2$ are generated. The two signal modes are degenerated in frequency but differ in the spatial mode, one (the other) corresponding to a Laguerre–Gauss mode with orbital angular momentum $l = +1$ ($l = -1$).

converted frequency, arriving to the same conclusion: Every time the nonlinear process generates light which breaks the rotational invariance of the system, the expected perfectly squeezed observable is found.

In the present paper we present a model for a $\chi^{(3)}$ –nonlinear cavity in which squeezing appears as the result of the rotational symmetry breaking. The interest of this new proposal is twofold. On one hand it allows us to demonstrate that rotational symmetry breaking is a robust means for generating squeezing in the sense that is not limited to a $\chi^{(2)}$ –nonlinear cavity such as the DOPO. On the other hand perfect rotational invariance could be problematic to achieve in $\chi^{(2)}$ systems because phase–matching requirements could imply the tilting of the nonlinear crystal thus compromising rotational invariance, a difficulty that disappears in a $\chi^{(3)}$ process because phase–matching occurs easily in this case.

The type of $\chi^{(3)}$ –nonlinear cavity system we are proposing here is a novel one that has not been studied previously, as far as we know. Hence we must derive the quantum model (Section II) as well as study its classical emission properties (Section III) before addressing its quantum properties (Section IV). We are able to demonstrate that the proposed device effectively exhibits perfect squeezing originating in the rotational symmetry breaking. In Section V we resume our main results.

II. MODEL

Consider an optical cavity with spherical mirrors containing an isotropic $\chi^{(3)}$ medium. The cavity is pumped from the outside with two coherent fields of frequencies ω_1 and ω_2 , these pumping beams having a Gaussian transverse profile. Suppose, for simplicity, that these pumping beams have the frequencies and shapes corresponding to two consecutive longitudinal modes of the optical cavity. Then, within the cavity the nonlinear interaction generates, through a four–wave mixing (FWM) process, two other fields having the same

frequency ω_s such that $\omega_1 + \omega_2 = 2\omega_s$. Assume now that the cavity geometry and tuning is such that these two signal fields have the shape of first order Laguerre–Gauss modes. These modes carry OAM and its conservation imposes that one of the signal fields carries positive OAM with $l = +1$ while the other carries negative OAM with $l = -1$ as the pumping fields have zero OAM (see Fig. 1).

As stated, the just described FWM process requires that the optical cavity modes, as well as the fields’ frequencies, be properly chosen. An immediate choice that verifies the previous requirements is a confocal resonator. In this type of cavity the resonance frequency of longitudinal mode q corresponding to the transverse family $f = 2p + l$ (p is the radial index) is given by [10]

$$\omega_{qf} = \frac{\pi c}{L} \left(q + \frac{1+f}{2} \right), \quad (1)$$

where L is the effective cavity length. In this case, the pumping beams can correspond to two consecutive longitudinal modes with $f = 0$. The signal modes would then correspond to the cavity modes with indices q and $f = 1$, as they verify $2\omega_s = \omega_{q,0} + \omega_{q+1,0} = 2\omega_{q,1}$. Certainly, in the confocal resonator there are other modes with frequency ω_s (an infinite number indeed) having larger odd angular momenta and belonging to other families. However we can neglect them by considering that these higher order Laguerre–Gauss modes could have larger cavity losses (what is true for low Fresnel number cavities) and would consequently not be amplified. Once we have shown that the FWM process we propose could be experimentally implemented, we pass to formulate the mathematical model of our system.

A. The fields

We shall assume for simplicity that the $\chi^{(3)}$ crystal is placed at the cavity’s waist plane and that is thin enough as to perform the uniform field approximation, hence neglecting any dependence of the fields on the axial coordinate z . Thus we write the total quantum field inside the cavity, at the beam waist, as

$$\hat{E}(\mathbf{r}, t) = \hat{E}_p(\mathbf{r}, t) + \hat{E}_s(\mathbf{r}, t), \quad (2a)$$

$$\hat{E}_p(\mathbf{r}, t) = \sum_{j=1,2} i\mathcal{F}_j \hat{A}_j(\mathbf{r}, t) e^{-i\omega_j t} + H.c., \quad (2b)$$

$$\hat{E}_s(\mathbf{r}, t) = i\mathcal{F}_s \hat{A}_s(\mathbf{r}, t) e^{-i\omega_s t} + H.c., \quad (2c)$$

where $H.c.$ stands for Hermitian conjugate; $\mathbf{r} = r(\cos\phi, \sin\phi)$ is the position vector in the transverse plane written in polar coordinates; subindices p and s denote pump and signal modes, respectively; $\mathcal{F}_k^2 = \hbar\omega_k/(\varepsilon_0 nL)$, with $k = 1, 2, s$; and n is the refractive index (we neglect dispersion for simplicity). The slowly varying amplitudes are

$$\hat{A}_j(\mathbf{r}, t) = \hat{a}_j(t) G_j(\mathbf{r}), \quad j = 1, 2, \quad (3a)$$

$$\hat{A}_s(\mathbf{r}, t) = \hat{a}_+(t) L_+(\mathbf{r}) + \hat{a}_-(t) L_-(\mathbf{r}), \quad (3b)$$

with $\hat{a}_k(t)$ and $\hat{a}_k^\dagger(t)$ the annihilation and creation operators for mode $k = 1, 2, +, -$, which verify $[\hat{a}_m(t), \hat{a}_n^\dagger(t)] = \delta_{mn}$.

As for the spatial dependence in (3), they are given by [10]

$$G_j(\mathbf{r}) = \sqrt{\frac{2}{\pi}} \frac{1}{w_j} e^{-(r/w_j)^2}, \quad j = 1, 2, \quad (4a)$$

$$L_{\pm 1}(\mathbf{r}) = \frac{2}{\sqrt{\pi}} \frac{r}{w_s^2} e^{-(r/w_s)^2} e^{\pm i\phi}, \quad (4b)$$

for the Gaussian and first order Laguerre–Gauss modes, respectively. In all cases $w_j \propto 1/\sqrt{\omega_j}$, $j = 1, 2, s$. Notice however that in the optical domain, in which $\omega_1 \sim 10^{15} \text{s}^{-1}$, one can safely take $\omega_1 \simeq \omega_2 \simeq \omega_s$ as far as L is not very small, which implies that the waist is very nearly the same for all of the involved modes. We make this approximation that, although not essential, simplifies some expressions below.

For later use we need the relation between the Laguerre–Gauss modes and the Hermite–Gauss modes

$$H_c^\sigma = \frac{e^{-i\sigma} L_{+1} + e^{i\sigma} L_{-1}}{\sqrt{2}} = \sqrt{2} |L_{\pm 1}(\mathbf{r})| \cos(\phi - \sigma), \quad (5a)$$

$$H_s^\sigma = \frac{e^{-i\sigma} L_{+1} - e^{i\sigma} L_{-1}}{i\sqrt{2}} = \sqrt{2} |L_{\pm 1}(\mathbf{r})| \sin(\phi - \sigma), \quad (5b)$$

being H_c^σ and H_s^σ the Hermite–Gauss modes with an orientation σ and $\sigma + \pi/2$ with respect to the x -axis, respectively. Thus the slowly varying amplitudes at frequency ω_s can also be written as

$$\hat{A}_s(\mathbf{r}, t) = \hat{a}_{c,\sigma}(t) H_c^\sigma + \hat{a}_{s,\sigma}(t) H_s^\sigma, \quad (6)$$

with

$$\hat{a}_{c,\sigma} = \frac{1}{\sqrt{2}} (e^{i\sigma} \hat{a}_+ + e^{-i\sigma} \hat{a}_-), \quad (7a)$$

$$\hat{a}_{s,\sigma} = \frac{i}{\sqrt{2}} (e^{i\sigma} \hat{a}_+ - e^{-i\sigma} \hat{a}_-), \quad (7b)$$

the annihilation operators for the Hermite–Gauss modes. Finally, we introduce the field quadratures of these Hermite–Gauss modes

$$\hat{X}_{j,\sigma}^\varphi = e^{-i\varphi} \hat{a}_{j,\sigma} + e^{i\varphi} \hat{a}_{j,\sigma}^\dagger, \quad j = c, s, \quad (8)$$

with $\hat{a}_{c,\sigma}$ and $\hat{a}_{s,\sigma}$ given by Eqs. (7).

B. The Hamiltonian

In the interaction picture, the system's Hamiltonian can be written as

$$\hat{H} = \hat{H}_0 + \hat{H}_{\text{ext}} + \hat{H}_{\text{int}}. \quad (9)$$

\hat{H}_0 and \hat{H}_{ext} correspond to the modes' energies and external injection, respectively, and are given by

$$\hat{H}_0 = \sum_{j=1,2,+,-} \hbar \delta_j a_j^\dagger a_j, \quad (10a)$$

$$\hat{H}_{\text{ext}} = i\hbar \mathcal{E}_1 (\hat{a}_1^\dagger - \hat{a}_1) + i\hbar \mathcal{E}_2 (\hat{a}_2^\dagger - \hat{a}_2), \quad (10b)$$

with $\delta_j = (\omega_{Cj} - \omega_j)$ the cavity detuning for the mode with frequency ω_j , being ω_{Cj} the cavity resonance closest to that mode. In a confocal resonator this detuning is the same for all the modes if the relative frequency of the pump modes is locked to the free spectral range of the cavity, i.e., $\omega_2 - \omega_1 =$

$\pi c/L$. Hence, in the following we take $\delta_j = \delta \forall j$. \mathcal{E}_j are the pumping parameters, which are related to the experimental parameters by

$$\mathcal{E}_j = \sqrt{\frac{c}{2\omega_j \hbar L} T(\omega_j) P_j},$$

being $T(\omega_j)$ the transmission factor at the considered frequency and P_j the power of the pumped laser. In the following we will assume $\mathcal{E}_1 = \mathcal{E}_2 = \mathcal{E}$ for simplicity. \hat{H}_{int} describes the nonlinear interaction and can be written as the sum of three contributions

$$\hat{H}_{\text{int}} = -\hbar g (\hat{H}_{\text{spm}} + \hat{H}_{\text{cpm}} + \hat{H}_{\text{fwm}}), \quad (11)$$

with

$$\hat{H}_{\text{spm}} = \hat{a}_1^{\dagger 2} \hat{a}_1^2 + \hat{a}_2^{\dagger 2} \hat{a}_2^2 + \frac{1}{2} (\hat{a}_+^{\dagger 2} \hat{a}_+^2 + \hat{a}_-^{\dagger 2} \hat{a}_-^2), \quad (12)$$

$$\hat{H}_{\text{cpm}} = 4\hat{a}_1^\dagger \hat{a}_1 \hat{a}_2^\dagger \hat{a}_2 + 2\hat{a}_+^\dagger \hat{a}_+ \hat{a}_-^\dagger \hat{a}_- + 2(\hat{a}_+^\dagger \hat{a}_1 + \hat{a}_2^\dagger \hat{a}_2) (\hat{a}_+^\dagger \hat{a}_+ + \hat{a}_-^\dagger \hat{a}_-), \quad (13)$$

$$\hat{H}_{\text{fwm}} = 2(\hat{a}_1^\dagger \hat{a}_2^\dagger \hat{a}_+ \hat{a}_- + \hat{a}_1 \hat{a}_2 \hat{a}_+^\dagger \hat{a}_-^\dagger), \quad (14)$$

describing self–phase modulation, cross–phase modulation, and four–wave mixing, respectively. Note that this Hamiltonian contains all the possible combinations of four operators conserving both energy and OAM. The factors multiplying the different terms are intuitive once one takes into account the two following features: (i), there is a global factor 4 in \hat{H}_{cpm} and \hat{H}_{fwm} with respect to \hat{H}_{spm} coming from all possible permutations of the different operators; and (ii), if any of the four modes is a signal mode, a factor 1/2 appears that comes from the transverse modes' overlapping integral. Finally, it can be shown that the coupling constant is given by

$$g = \frac{6\mathcal{F}^4 \varepsilon_0 l_c \chi}{\pi \hbar w^2}, \quad (15)$$

with w the beam waist, l_c the crystal length and χ the third-order nonlinear susceptibility of the crystal.

C. The quantum evolution equations

In this subsection we apply the standard procedure to develop the quantum theory of a nonlinear resonator within the generalized P representation to our Kerr cavity model [11], [12], [13]. The starting point is the system's master equation for the density operator $\hat{\rho}$, which reads

$$\frac{d}{dt} \hat{\rho} = \frac{1}{i\hbar} [\hat{H}, \hat{\rho}] + \widehat{\mathcal{L}} \hat{\rho}, \quad (16)$$

where $\widehat{\mathcal{L}}$ is the Liouvillian superoperator describing field losses through the output mirror, which applied to the density operator reads

$$\widehat{\mathcal{L}} \hat{\rho} = \sum_{j=1,2,+,-} \gamma_j \left([\hat{a}_j, \hat{\rho} \hat{a}_j^\dagger] + [\hat{a}_j \hat{\rho}, \hat{a}_j^\dagger] \right). \quad (17)$$

As we are assuming that the system has perfect rotational symmetry around the cavity axis it follows that $\gamma_+ = \gamma_- \equiv \gamma_s$.

As usual, we use now the generalized P representation in order to transform the operator master equation into a partial

differential equation for the quasiprobability distribution P . In this representation, to every pair of boson operators $(\hat{a}_j, \hat{a}_j^\dagger)$ it corresponds a pair of independent stochastic amplitudes (α_j, α_j^+) verifying $\langle \alpha_j^+ \rangle = \langle \alpha_j \rangle^*$. By using standard techniques, one finds that the Fokker–Planck equation governing the evolution of P reads

$$\frac{\partial}{\partial t} P(\boldsymbol{\alpha}; t) = \left[-\frac{\partial}{\partial \alpha_i} A_i + \frac{1}{2} \frac{\partial^2}{\partial \alpha_i \partial \alpha_j} \mathcal{D}_{ij} \right] P(\boldsymbol{\alpha}; t), \quad (18)$$

where we write vector $\boldsymbol{\alpha}$ as

$$\boldsymbol{\alpha} = (\alpha_1, \alpha_2, \alpha_+, \alpha_-, \alpha_1^+, \alpha_2^+, \alpha_+^+, \alpha_-^+), \quad (19)$$

and give the explicit expression of the components of both the drift vector $\mathbf{A}(\boldsymbol{\alpha})$ and the diffusion matrix $\mathcal{D}(\boldsymbol{\alpha})$ in Appendix A.

Once the Fokker–Planck equation is known, it can be converted, by applying Ito rules, into an equivalent set of stochastic first-order differential equations: The quantum Langevin equations. They read

$$\frac{d}{dt} \boldsymbol{\alpha} = \mathbf{A}(\boldsymbol{\alpha}) + \mathcal{B}(\boldsymbol{\alpha}) \cdot \boldsymbol{\eta}(t) \quad (20)$$

where the components of $\boldsymbol{\eta}(t)$ are real gaussian noises verifying

$$\langle \eta_i(t) \rangle = 0, \quad (21a)$$

$$\langle \eta_i(t) \eta_j(t') \rangle = \delta_{ij} \delta(t - t'), \quad (21b)$$

and the noise matrix \mathcal{B} can be obtained from

$$\mathcal{D} = \mathcal{B} \cdot \mathcal{B}^T. \quad (22)$$

The equivalency between the master equation and Langevin equations must be understood as follows

$$\langle : f(\hat{a}_m, \hat{a}_m^\dagger) : \rangle = \langle f(\alpha_m, \alpha_m^+) \rangle_{stochastic}, \quad (23)$$

i.e., quantum expected values of normally ordered functions are equal to the stochastic averages of the same functions after changing boson operators $(\hat{a}_m, \hat{a}_m^\dagger)$ by independent complex stochastic variables (α_m, α_m^+) .

With this procedure, we have obtained a set of stochastic differential equations, Eqs. (20) together with Eqs. (64) and (66), ruling the evolution of the fields inside the cavity. However, the analysis of this model turns out to be quite involved.

A simpler model retaining the essential ingredients consists in neglecting the temporal evolution of the pumping fields, or further, considering the undepletion limit for the pump. As follows from (64a) and (64b) applied to (20), this will be a reasonable approximation whenever the gain g , Eq. (15), is small enough as for $|\alpha_\pm| \ll |\alpha_{1,2}|$. In such a case one can safely neglect the amplitude variation of the pump modes. Of course, in doing that some of the dynamical richness of the system is lost, but the approximation simplifies very much the analysis of the rotational symmetry breaking which is fully retained by the simplified model.

Hence, in the following we will study a reduced model in which the pump fields are taken to be equal (and real without loss of generalization), i.e., we take

$$\alpha_1 = \alpha_2 \equiv \rho \in \mathbb{R}. \quad (24)$$

D. The reduced model

Under the assumption that the pump fields remain constant, thus satisfying (24), the Fokker–Planck equation of the system looks like Eq. (18), but with simpler diffusion matrix and drift vector.

From the general expressions given in Appendix A it is easy to obtain that the diffusion matrix reads now

$$\mathcal{D} = \begin{pmatrix} \mathcal{D}^{(-)} & 0 \\ 0 & \mathcal{D}^{(+)} \end{pmatrix}, \quad (25a)$$

$$\mathcal{D}^{(-)} = ig \begin{pmatrix} \alpha_+^2 & 2\alpha_+ \alpha_- + 2\rho^2 \\ 2\alpha_+ \alpha_- + 2\rho^2 & \alpha_-^2 \end{pmatrix}, \quad (25b)$$

($\mathcal{D}^{(+)}$ is like $\mathcal{D}^{(-)}$ but swapping α_k and α_k^+ , and changing i by $-i$), and that the components of the drift vector are

$$A_{\alpha_\pm} = -(\gamma_s + i\delta) \alpha_\pm + i(\alpha_\pm^+ \alpha_\pm + 2\alpha_\mp^+ \alpha_\mp + 4\rho^2) \alpha_\pm + 2i\rho^2 \alpha_\mp^+, \quad (26)$$

being $A_{\alpha_\pm^+}$ like A_{α_\pm} after swapping α_k and α_k^+ , and changing i by $-i$.

Like before, from this Fokker–Planck equation, a set of Langevin equations can be obtained. Nevertheless, it will be useful to introduce the following change of variables and parameters (we note that the phase factor ψ appearing in the rescaled fields is introduced to make the stationary solutions of the classical equations satisfy $\beta_- = \beta_+^*$, see Eqs. (33), which simplifies the quantum analysis)

$$\beta_\pm = \sqrt{\frac{g}{\gamma_s}} \alpha_\pm e^{-i\psi}, \quad \beta_\pm^+ = \sqrt{\frac{g}{\gamma_s}} \alpha_\pm^+ e^{i\psi}, \quad (27)$$

$$p = 2\frac{g}{\gamma_s} \rho^2, \quad \Delta = \frac{\delta}{\gamma_s}, \quad \kappa = \frac{g}{\gamma_s}, \quad T = \gamma_s t$$

with

$$\sin 2\psi = \sqrt{\frac{\gamma_s}{g}} \frac{1}{2\rho} = \frac{1}{\sqrt{2p}}, \quad (28)$$

in terms of which the Langevin equations for the reduced model read

$$\dot{\beta}_\pm = -(1 + i\Delta) \beta_\pm + i(\beta_\pm^+ \beta_\pm + 2\beta_\mp^+ \beta_\mp + 2p) \beta_\pm + ipe^{-2i\psi} \beta_\mp^+ + \tilde{\mathcal{B}}_{\beta_\pm, j} \xi_j(T), \quad (29)$$

plus the corresponding equations for β_\pm^+ which are like those for β_\pm above after swapping β_k and β_k^+ , and changing i by $-i$. The overdot indicates derivative with respect to the adimensional time T , and the four components of the noise vector $\boldsymbol{\xi}$ satisfy properties (21) now for the adimensional time T . As for the noise matrix $\tilde{\mathcal{B}}$, it can be obtained from $\tilde{\mathcal{D}} = \tilde{\mathcal{B}} \cdot \tilde{\mathcal{B}}^T$ as usual, but now using the diffusion matrix after introducing the changes (27), which reads as (25a) but with

$$\tilde{\mathcal{D}}^{(-)} = ig \begin{pmatrix} \alpha_+^2 & 2\alpha_+ \alpha_- + 2e^{-2i\psi} \rho^2 \\ 2\alpha_+ \alpha_- + 2e^{-2i\psi} \rho^2 & \alpha_-^2 \end{pmatrix},$$

and with $\mathcal{D}^{(+)}$ like $\mathcal{D}^{(-)}$ but swapping α_k and α_k^+ , and changing i by $-i$. In any case, there is no need to evaluate $\tilde{\mathcal{B}}$ at this moment.

Eqs. (29) constitute the model we analyze in detail below.

III. CLASSICAL LIMIT

Before addressing the analysis of quantum fluctuations we need to know the classical steady states of the system as well as their stability properties, and for doing that we must first write down the classical limit of Eqs. (29). This is easily done by neglecting the noise terms and by making $\beta_j^+ = \beta_j^*$ in the quantum Langevin Eqs. (29). We obtain the following set of two complex ordinary differential equations for the signal classical fields amplitudes β_{\pm} :

$$\dot{\beta}_{\pm} = - \left[1 + i \left(\Delta - |\beta_{\pm}|^2 - 2|\beta_{\mp}|^2 - 2p \right) \right] \beta_{\pm} + i p e^{-2i\psi} \beta_{\mp}^* \quad (30)$$

Thanks to rescaling (27) we can appreciate that the classical dynamics of the system is governed by just two parameters, namely the normalized detuning Δ and pump strength p . We pass now to study the stationary solutions of Eqs. (30) as well as their stability properties.

Eqs. (30) have two steady states. First there is the trivial steady state $\beta_{\pm} = 0$. It is easy to show that its stability is governed by the eigenvalues

$$\lambda_{\pm} = -1 \pm \sqrt{p^2 - (\Delta - 2p)^2}, \quad (31)$$

what implies that the trivial solution is stable except when the pump amplitude p verifies $p_- < p < p_+$ with

$$p_{\pm} = \frac{1}{3} \left(2\Delta \pm \sqrt{\Delta^2 - 3} \right), \quad (32)$$

in which case the trivial solution becomes linearly unstable because $\text{Re}(\lambda_+) > 0$. Notice that a prerequisite for the destabilization of the trivial solution is that $\Delta > \sqrt{3}$ (p is positive).

At the instability points $\text{Re}(\lambda_+) = 0$ the system passes from the trivial state to the nontrivial one, which reads

$$\bar{\beta}_{\pm} = \mu e^{\mp i\theta}, \quad (33)$$

with

$$\mu^2 = \frac{1}{3} \left(\Delta - 2p \pm \sqrt{p^2 - 1} \right), \quad (34)$$

and where θ is half the phase-difference between the two Laguerre–Gauss modes amplitudes, and is not fixed by Eqs. (30), being hence arbitrary. In Fig. 2(a) this solution is shown as a function of p for three values of Δ .

Notice first that there are two possible values for μ . It is easy to demonstrate that the solution with the minus sign in front of the square root (dashed lines in Fig. 2(a)) is always unstable, while the solution with the plus sign (continuous lines in Fig. 2(a)) is stable within all its domain of existence. Notice also that while the sum of the phases of the two Laguerre–Gauss modes amplitudes is fixed to zero (this is thanks to the change of variables (27)), their phase difference θ is an arbitrary quantity, which reflects the rotational invariance of the system as this phase difference determines the orientation in the transverse plane of the emitted Hermite–Gauss mode, see Eq. (36) below.

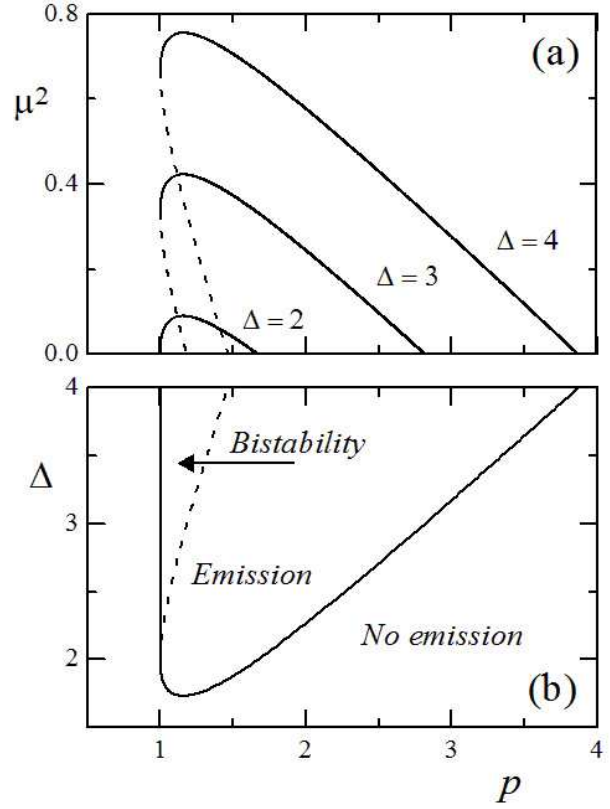


Figure 2.- (a) Intensity of the emitted classical signal beam as a function of the pump strength p for the indicated values of the detuning Δ . Continuous (dashed) lines indicate linearly stable (unstable) solutions. (b) Domain of existence and stability of the solutions. The non trivial solution exists in the domain limited by the two continuous lines. The trivial solution is stable to the left of the dashed line and to the right of the right continuous line. Hence, the system is bistable in the region between the dashed line and the left continuous line, marked in the figure.

From Eq. (34) it follows that the necessary condition for the existence of the nontrivial solution is $p > 1$, and its domain of existence is determined by the condition

$$\Delta > 2p - \sqrt{p^2 - 1}. \quad (35)$$

Note that this inequality can be satisfied only if $\Delta > \sqrt{3}$, in agreement with our analysis of the trivial solution. In Fig. 2(b) we represent this domain of existence as well as the domain of stability of the trivial solution, see Fig. 2(b) caption.

From all the above we see that the classical nontrivial state slowly-varying amplitude can be written as

$$A_s^{class}(\mathbf{r}) = \mu \left[e^{-i\theta} L_+(\mathbf{r}) + e^{+i\theta} L_-(\mathbf{r}) \right] = \left[\frac{2}{3} \left(\Delta - 2p + \sqrt{p^2 - 1} \right) \right]^{1/2} H_c^\theta(\mathbf{r}). \quad (36)$$

This solution corresponds to a Hermite–Gauss mode rotated an angle θ with respect to the x -axis, being the value of this angle arbitrary. As already noticed, the arbitrariness of θ is the consequence of the rotational symmetry of the system: As the pumping modes are rotationally symmetric, as the cavity is, the signal TEM_{10} Hermite–Gauss mode cannot have

any preferred orientation and thus all orientations are equally likely. This property is essential for the results we present below for quantum fluctuations.

Finally, note that the fact that the emission takes place in a TEM₁₀ mode, allows us to distinguish between two different modes: The $H_c^\theta(\mathbf{r})$ mode, which is the classically generated one, and its orthogonal mode $H_s^\theta(\mathbf{r})$, which is empty of photons at the classical level. In the following we shall refer to these modes as the *bright* and *dark* modes, respectively.

IV. QUANTUM ANALYSIS

We return to the quantum description of the system. In the following subsections we first derive the linearized Langevin equations and then solve them with the method introduced in [14], [15] and further used in [7], [8], [9]. Next we show the most outstanding quantum properties of the system: After proving that the bright mode is rotating randomly in the transverse plane, we show that the dark mode has perfect noise reduction in one of its quadratures.

A. Linearization of the Langevin equations

We linearize Eqs. (29), a valid approximation in the large photon number limit and thus appropriate for our purposes as we are going to analyze quantum fluctuations around the above threshold solution (33). Consequently we write

$$\beta_\pm = [\mu + b_\pm(T)] e^{\mp i\theta(T)}, \quad (37a)$$

$$\beta_\pm^\dagger = [\mu + b_\pm^\dagger(T)] e^{\pm i\theta(T)}, \quad (37b)$$

where the phase difference θ appears explicitly in order to keep the b 's small. Then, by assuming that b_j , ξ_j , and θ are small quantities, we easily arrive to the following linearized Langevin equations

$$\dot{\mathbf{b}} + iN_0\mu\dot{\theta}\mathbf{v}_0 = \mathcal{L}\mathbf{b} + \mathcal{K}\bar{\mathcal{B}}\boldsymbol{\xi} \quad (38)$$

where

$$\mathbf{b} = \text{col}(b_+, b_-, b_+^\dagger, b_-^\dagger), \quad (39a)$$

$$\mathbf{v}_0 = \frac{1}{N_0} \text{col}(-1, 1, 1, -1), \quad (39b)$$

N_0 is a normalization factor (see Eq. (49) below), \mathcal{L} is a matrix with elements

$$\mathcal{L}_{ij} = \left. \frac{\partial A_i}{\partial \beta_j} \right|_{\beta=\bar{\beta}}, \quad (40)$$

and \mathcal{K} is the diagonal matrix

$$\mathcal{K} = \text{diag}(e^{i\theta}, e^{-i\theta}, e^{-i\theta}, e^{i\theta}). \quad (41)$$

Finally, $\bar{\mathcal{B}}$ refers to matrix $\tilde{\mathcal{B}}$ evaluated at the stationary state (33). Its expression can be derived from $\bar{\mathcal{D}} = \tilde{\mathcal{B}} \cdot \tilde{\mathcal{B}}^T$ with

$$\bar{\mathcal{D}} = \tilde{\mathcal{D}} \Big|_{\beta=\bar{\beta}} = \begin{pmatrix} \bar{\mathcal{D}}^{(-)} & 0 \\ 0 & \bar{\mathcal{D}}^{(+)} \end{pmatrix}, \quad (42a)$$

$$\bar{\mathcal{D}}^{(-)} = [\bar{\mathcal{D}}^{(+)}]^* = i\kappa \begin{pmatrix} \mu^2 e^{-2i\theta} & 2\mu^2 + p e^{-2i\psi} \\ 2\mu^2 + p e^{-2i\psi} & \mu^2 e^{2i\theta} \end{pmatrix}. \quad (42b)$$

After some algebra, it is easy to show that $\bar{\mathcal{B}}$ can be written as

$$\bar{\mathcal{B}} = \begin{pmatrix} \bar{\mathcal{B}}^{(-)} & 0 \\ 0 & \bar{\mathcal{B}}^{(+)} \end{pmatrix}, \quad (43a)$$

$$\bar{\mathcal{B}}^{(-)} = [\bar{\mathcal{B}}^{(+)}]^* = \begin{pmatrix} a e^{-i\theta} & b e^{-i\theta} \\ c e^{i\theta} & d e^{i\theta} \end{pmatrix}, \quad (43b)$$

where elements (a, b, c, d) are independent of θ , and satisfy the following relations

$$a^2 + b^2 = c^2 + d^2 = i\kappa\mu^2, \quad (44a)$$

$$ac + bd = i\kappa(2\mu^2 + p e^{-2i\psi}). \quad (44b)$$

B. Solving the linearized Langevin equations

In order to solve the linearized Langevin Eqs. (38) we follow a procedure analogous to that in [7], [8], [9], [14], [15]. The method consists in projecting Eqs. (38) into the eigensystem of the linear operator \mathcal{L} . This provides a direct way for the evaluation of the quantum fluctuations of the relevant physical quantities, as we show below.

Operator \mathcal{L} has not an orthonormal but a biorthonormal eigensystem, i.e., there is an eigensystem of operators \mathcal{L} and \mathcal{L}^\dagger verifying

$$\mathcal{L}\mathbf{v}_j = \lambda_j\mathbf{v}_j, \quad \mathcal{L}^\dagger\mathbf{w}_j = \lambda_j^*\mathbf{w}_j, \quad (45a)$$

such that

$$\mathbf{w}_m^* \cdot \mathbf{v}_n = \delta_{mn}. \quad (46)$$

The quantitative result of the analysis of \mathcal{L} and \mathcal{L}^\dagger is that their four eigenvalues read

$$\lambda_0 = 0, \quad \lambda_1 = -2, \quad (47a)$$

$$\lambda_2 = \lambda_2(p, \Delta), \quad \lambda_3 = -2 - \lambda_2. \quad (47b)$$

We see that eigenvalue λ_0 is always null. This means that its corresponding eigenvector, which is said to be a Goldstone mode (its expression is given below), is neutrally stable, i.e., that its associated variable can take any possible value. Of course this reflects the indeterminacy of the phase difference between the two Laguerre–Gauss modes, θ , or what is the same, the indeterminacy of the orientation of the Hermite–Gauss output mode in the transverse plane. Hence, the null eigenvalue implies that the fluctuations introduced by quantum noise in this orientation are not damped and, hence, that quantum noise will induce arbitrary rotations of the Hermite–Gauss output mode in the transverse plane. Thus the breaking of the rotational symmetry of the system introduced by the appearance of the Hermite–Gauss mode is, in a sense, counteracted by quantum noise by making possible any possible orientation. Together with $\lambda_0 = 0$, there is the companion eigenvalue $\lambda_1 = -2$. Its corresponding eigenvector (see below) is consequently maximally damped irrespective of the system's parameter values. As we show below, it is the observable associated to the eigenvector corresponding to λ_1 the one that is perfectly squeezed.

On the other hand, the two other eigenvalues, λ_2 and λ_3 , are complex in general; nevertheless, they reach the values 0 and -2 at the bifurcation points (i.e., at the points in the parameter

space separating the regions where the steady state solution (33) exist or not). Consequently, their associated eigenvectors are those exhibiting the usual squeezing occurring only at the bifurcations. This squeezing is not perfect (it seems perfect only owed to the linearized treatment) and degrades quickly as the system parameters are brought apart from the bifurcation points. We shall not analyze this squeezing here because there is not any relevant new feature in it with respect to what has been described many times in other nonlinear optical cavities. Hence, in the following, we concentrate on the analysis of the modes associated to the first two eigenvalues that are the ones connected with the rotational symmetry breaking.

It is not difficult to show that the eigenvectors of \mathcal{L} associated to λ_0 and λ_1 are

$$\mathbf{v}_0 = \frac{1}{N_0} \text{col}(-1, 1, 1, -1), \quad (48a)$$

$$\mathbf{v}_1 = \frac{1}{N_0} \text{col}(e^{i\phi_0}, -e^{i\phi_0}, e^{-i\phi_0}, -e^{-i\phi_0}), \quad (48b)$$

with

$$N_0 = -4 \cos \phi_0, \quad (49)$$

a normalization factor and ϕ_0 a real quantity given by

$$e^{2i\phi_0} = \frac{\mu^2 + pe^{-i\psi}}{2(\mu^2 + p) - (\Delta + i)}. \quad (50)$$

As for the eigenvectors of \mathcal{L}^\dagger they read

$$\mathbf{w}_0 = \text{col}(e^{i\phi_0}, -e^{i\phi_0}, -e^{-i\phi_0}, e^{-i\phi_0}), \quad (51a)$$

$$\mathbf{w}_1 = \text{col}(1, -1, 1, -1). \quad (51b)$$

Once these eigenvectors of the linear operator are known, we proceed to project quantum fluctuations onto them. We define projections

$$c_j = \mathbf{w}_j^* \cdot \mathbf{b}, \quad j = 0, 1. \quad (52)$$

Note that these projections can be easily related with the fluctuations of the quadratures associated to modes H_c^σ and H_s^σ , see Eqs. (8). In particular, by using (8) and (37) it is easy to arrive at

$$X_{s,\theta}^{\phi_0} = \frac{i}{\sqrt{2}} c_0, \quad X_{s,\theta}^{\pi/2} = \frac{1}{\sqrt{2}} c_1. \quad (53)$$

Next we project the linearized Langevin Eqs. (38). By multiplying them by \mathbf{w}_j^* on the left we get

$$\dot{\theta}(T) = \frac{1}{iN_0\mu} \mathbf{w}_0^* \mathcal{K} \bar{\mathcal{B}} \boldsymbol{\xi}(T), \quad (54a)$$

$$\dot{c}_1(T) = \lambda_1 c_1(T) + \mathbf{w}_1^* \mathcal{K} \bar{\mathcal{B}} \boldsymbol{\xi}(T), \quad (54b)$$

where we have taken $c_0 = 0$ (this can be done because the arbitrary phase θ can be conveniently redefined in order to collect the information on this mode). We notice that although \mathcal{K} and $\bar{\mathcal{B}}$ depend on phase θ , $\mathcal{K} \bar{\mathcal{B}}$ does not as can be checked from Eqs. (41) and (43). Hence these equations are truly decoupled for θ and c_1 .

In the stationary limit, i.e. for large T , the solution of the above equations reads

$$\theta(T) = \theta(0) + \frac{\mathbf{w}_0^* \mathcal{K} \bar{\mathcal{B}}}{iN_0\mu} \int_0^T dT' \boldsymbol{\xi}(T'), \quad (55a)$$

$$c_1(T) = \mathbf{w}_1^* \mathcal{K} \bar{\mathcal{B}} \int_0^T dT' \boldsymbol{\xi}(T') e^{-2(T'-T)}. \quad (55b)$$

Finally we evaluate, for later purposes, the correlation spectrum of c_1 . From the formal solution (55b), it is straightforward to prove that the correlation function of this projection reads

$$C_1(\tau) = \langle c_1(T) c_1(T + \tau) \rangle = \frac{\mathbf{w}_1^* \mathcal{K} \bar{\mathcal{D}} \mathcal{K} \mathbf{w}_1^*}{4} e^{-2|\tau|}. \quad (56)$$

It is not difficult to obtain that $\mathbf{w}_1^* \mathcal{K} \bar{\mathcal{D}} \mathcal{K} \mathbf{w}_1^* = -4\kappa$, and then the spectrum of correlation $C_1(\tau)$ turns out to be

$$\tilde{C}_1(\omega) = \int_{-\infty}^{+\infty} d\tau e^{-i\omega\tau} C_1(\tau) = -\frac{\kappa}{4 + \omega^2}. \quad (57)$$

C. Dynamics of the bright mode's orientation

We first analyze the dynamics of the output pattern orientation, governed by θ . Eq. (58a) shows that the phase θ diffuses with time what means that the orientation of the classical mode in which emission occurs, Eq. (36), exhibits a random walk. Then, although the mode orientation is well defined at every instant, it can be understood that the pattern orientation is undefined as after some time any value between 0 and 2π could be found. This is what we understand when we say that the orientation of the output pattern is undetermined.

It is important to see how much does θ diffuse. From Eq. (55a) it is straightforward to show that the variance of θ is given by

$$\langle \delta\theta(T)^2 \rangle = d_\theta T, \quad (58a)$$

where we have used the notation $\delta A = A - \langle A \rangle$, and

$$\begin{aligned} d_\theta &= -\frac{\mathbf{w}_0^* \mathcal{K} \bar{\mathcal{D}} \mathcal{K} \mathbf{w}_0^*}{N_0^2 \mu^2} \\ &= \kappa \frac{\mu^2 \sin 2\phi_0 + p \sin [2(\phi_0 + \psi)]}{4\mu^2 \cos^2 \phi_0}, \end{aligned} \quad (59)$$

with ψ , μ , and ϕ_0 given by Eqs. (28), (34) and (50).

In Fig. 3 we represent $D \equiv d_\theta/\kappa$ as a function of the pump strength p for several values of Δ . Notice that for $\mu \rightarrow 0$ (i.e., at the supercritical bifurcation that occurs in the upper branch of the domain of existence of (33), see Fig. 2), $D \rightarrow \infty$. This is an intuitive result because when the output mode mean photon number is close to zero, the pattern orientation can be abruptly changed with the addition of a single couple of photons. As the system is brought apart from this bifurcation the mean number of photons rapidly increases and, consequently, it is more difficult for the fluctuation to change the orientation of the pattern, what is obviously consistent with the rapid decrease of D . As for the quantitative value notice that, except very close to the supercritical bifurcations, D is a quantity of order one what means that the diffusion constant d_θ is basically of the

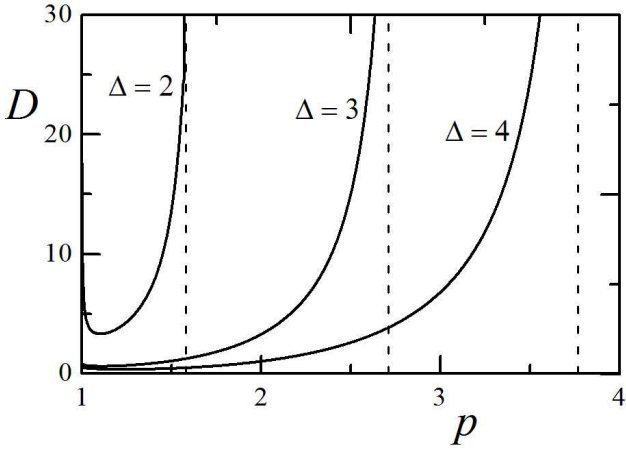


Figure 3.- Dependence of the normalized diffusion constant $D = d_\theta/\kappa$ as a function of the pump strength p for the values of the detuning indicated in the figure. The vertical dashed lines indicate the values of p where the nontrivial solution ceases to exist.

same order of magnitude as $\kappa = g/\gamma_s$, which we have assumed to be a very small number. Consequently, although the TEM output mode is randomly rotating in the transverse plane, the rotation is very slow except very close to the supercritical bifurcation points.

D. Non-critical squeezing properties of the dark mode

Now we focus on the main result of the present article: We show below that the dark mode has complete noise reduction on its phase quadrature irrespective of the system parameters. To this aim we evaluate its quadrature fluctuations as measured in an homodyne detection experiment. As it is well known (see, e.g., [16]), quadrature fluctuations outside the cavity are given by the noise spectrum, which for a general problem quadrature \hat{X}_m^φ (m refers to any of the transverse modes of our system) is given by

$$V^{out}(\omega; X_m^\varphi) = 1 + S_m^\varphi(\omega), \quad (60)$$

with $S_m^\varphi(\omega)$ the squeezing spectrum that, after taking into account our rescaling (27), can be written as

$$S_m^\varphi(\omega) = \frac{2}{g} \int_{-\infty}^{+\infty} d\tau e^{-i\omega\tau} \langle \delta X_m^\varphi(T) \delta X_m^\varphi(T+\tau) \rangle. \quad (61)$$

Defined in this way, $V^{out}(\bar{\omega}) = 0$ means complete absence of fluctuations at $\omega = \bar{\omega}$, while $V^{out}(\bar{\omega}) = 1$ means that fluctuations at $\omega = \bar{\omega}$ are those corresponding to the vacuum state.

In the homodyning, the spatial profile of the local oscillator field (LOF) selects the transverse mode to be measured, while its phase selects a particular mode's quadrature. In what follows we suppose that the LOF is perfectly matched to the dark mode's profile $H_s^\theta(\mathbf{r})$. As we saw in (53), the independent quadratures of this mode are $X_{s,\theta}^{\phi_0}$ and $X_{s,\theta}^{\pi/2}$, from which we can build a general quadrature as

$$X_{s,\theta}^\varphi = \frac{1}{\cos\phi_0} \left[X_{s,\theta}^{\phi_0} \cos\varphi + Y_{s,\theta} \sin(\varphi - \phi_0) \right]. \quad (62)$$

This expression is readily obtained from the more common expressions $X_{s,\theta}^\varphi = X_{s,\theta}^0 \cos\varphi + X_{s,\theta}^{\pi/2} \sin\varphi$ and $X_{s,\theta}^{\phi_0} = X_{s,\theta}^0 \cos\phi_0 + X_{s,\theta}^{\pi/2} \sin\phi_0$.

Hence, by using the relation between the independent quadratures and the projections c_j (53), and remembering Eq. (57) and that $c_0 = 0$, it is trivial to find the noise spectrum of this general quadrature, which reads

$$V^{out}(\omega; X_{s,\theta}^\varphi) = \frac{\cos^2\varphi + \sin^2(\varphi - \phi_0)}{\cos^2\phi_0} - \frac{\sin^2(\varphi - \phi_0)}{\cos^2\phi_0} \frac{1}{1 + (\omega/2)^2}. \quad (63)$$

This expression shows that the quantum properties of the dark mode of the current system are exactly the same as that found in [7], [8] for the case of a DOPO cavity: at $\omega = 0$, $V^{out}(\omega = 0; X_{s,\theta}^\varphi) = \cos^2\varphi/\cos^2\phi_0$ and thus it has complete absence of fluctuations on its phase quadrature ($\varphi = \pi/2$), while another of its quadratures ($\varphi = \phi_0$ in our case) carries only with vacuum fluctuations. Any other quadrature having φ between $\pi/2$ and ϕ_0 is squeezed below the vacuum level, though the squeezing level is smaller as φ approaches to ϕ_0 . These results are independent of the system parameters, what we expected as the noise reduction relies on the rotational symmetry breaking only.

It could seem that this result violates the uncertainty principle, as the product of the noise spectra corresponding to two orthogonal quadratures is below unity. However, in [8], we have proven that this is actually not the case, as the canonical pair of the squeezed quadratures is not another quadrature, but the orientation of the dark mode θ , which is indeed undetermined in the long time term.

V. CONCLUSIONS

We have proposed a model for a Kerr cavity in which a spontaneous rotational symmetry breaking occurs when the system is beyond the emission threshold: The nonlinear cavity has a perfect rotational symmetry and is pumped by Gaussian beams, but the emitted signal field has the shape of a TEM₁₀ mode that breaks the rotational symmetry. We have demonstrated in a special simple limit (in which the pumping fields are taken as constants) that the rotational symmetry breaking implies (i) the diffusion of the output mode orientation, and (ii) the perfect squeezing of the phase quadrature of the TEM₁₀ mode that is rotated $\pi/2$ with respect to the signal TEM₁₀ mode. These results are in perfect agreement with our previous proposal of the symmetry breaking mediated squeezing in a DOPO model [7], [8]. The interest of the results here presented are twofold. On one hand, we are proposing a system different to that of [7], [8] for the possible observation of the phenomenon, thus showing that the results in [7], [8] are quite general. On the other hand, rotational symmetry could be broken in a DOPO cavity if angular phase matching is necessary, as in this case the nonlinear crystal axis is rotated a certain angle with respect to the cavity axis, a problem that does not exist in the case of a $\chi^{(3)}$ nonlinear medium as phase matching is easier to obtain.

As for the particular model we have proposed, in its formulation we have assumed a confocal cavity, as in this cavity type the required resonances are verified. Notice however that the ingredients that are essential for the phenomenon of rotational symmetry breaking mediated squeezing generation are: (i) rotational invariance, and (ii) that the signal field photons have non-null OAM. Then, the dynamics of the pumping modes is irrelevant except for the quantitative details. In this sense, the use of a confocal cavity is not essential and any other $\chi^{(3)}$ cavity in which the signal modes are the right ones could exhibit the described phenomenon. Then this phenomenon could possibly be observed in other $\chi^{(3)}$ cavities such as, e.g., fiber ring resonators.

Another comment we would like to add concerns the non-pump depletion approximation. How would the dynamics of the pumping modes affect the results we have derived? The inclusion of the pumping fields equations in the study would obviously introduce more eigenvalues (the ones corresponding to the stability of these modes) and would modify some of the eigenvalues governing the dynamics of the signal modes, but would not modify the existence of a Goldstone mode once the signal field is switched on (as it appears due to the symmetry breaking). Hence as far as the dynamics of the pumping modes does not destroy completely the stability of the cw signal field emission, wherever the signal modes are stable the phenomenon will be present. It could well happen that the general model exhibits Hopf bifurcations that would reduce the domain of stable existence of the cw signal modes, but there will be a finite domain of stability for these modes and within it there will be the perfect squeezing properties we have described in our work.

We would finally stress two important features. In [7] we demonstrated for a DOPO model that small imperfections in the rotational symmetry do not lead but to a small degradation of the squeezing level. On the other hand, in [8] we have numerically demonstrated for the same DOPO model that the rotational symmetry breaking mediated squeezing is perfect beyond the linear approximation. These conclusions should also hold for the system here presented.

APPENDIX

The components of the drift vector in Eq. (18) read

$$A_{\alpha_1} = \mathcal{E}_p - (\gamma_1 + i\delta) \alpha_1 + 4ig\alpha_2^+ \alpha_2 \alpha_1 + 2ig(\alpha_1^+ \alpha_1^2 + \alpha_+^+ \alpha_+ \alpha_1 + \alpha_-^+ \alpha_- \alpha_1 + \alpha_2^+ \alpha_+ \alpha_-), \quad (64a)$$

$$A_{\alpha_2} = \mathcal{E}_p - (\gamma_2 + i\delta) \alpha_2 + 4ig\alpha_1^+ \alpha_1 \alpha_2 + 2ig(\alpha_2^+ \alpha_2^2 + \alpha_+^+ \alpha_+ \alpha_2 + \alpha_-^+ \alpha_- \alpha_2 + \alpha_1^+ \alpha_+ \alpha_-), \quad (64b)$$

$$A_{\alpha_+} = -(\gamma_s + i\delta) \alpha_+ + ig\alpha_+^+ \alpha_+^2 + 2ig(\alpha_-^+ \alpha_- \alpha_+ + \alpha_1^+ \alpha_1 \alpha_+ + \alpha_2^+ \alpha_2 \alpha_+ + \alpha_-^+ \alpha_1 \alpha_2), \quad (64c)$$

$$A_{\alpha_-} = -(\gamma_s + i\delta) \alpha_- + ig\alpha_-^+ \alpha_-^2 + 2ig(\alpha_+^+ \alpha_+ \alpha_- + \alpha_1^+ \alpha_1 \alpha_- + \alpha_2^+ \alpha_2 \alpha_- + \alpha_+^+ \alpha_1 \alpha_2), \quad (64d)$$

and the rest of components $A_{\alpha_k^+}$ are as A_{α_k} after complex-conjugating and swapping α_k and α_k^+ . As for the diffusion matrix in Eq. (18), it reads

$$D = 2ig \begin{pmatrix} \mathcal{D}^{(-)} & 0 \\ 0 & -\mathcal{D}^{(+)} \end{pmatrix}, \quad (65)$$

being $\mathcal{D}^{(-)}$ a 4×4 matrix with elements

$$\mathcal{D}_{11}^{(-)} = \alpha_1^2, \mathcal{D}_{22}^{(-)} = \alpha_2^2, \mathcal{D}_{33}^{(-)} = \frac{\alpha_+^2}{2}, \mathcal{D}_{44}^{(-)} = \frac{\alpha_-^2}{2}, \quad (66a)$$

$$\mathcal{D}_{12}^{(-)} = \mathcal{D}_{21}^{(-)} = 2\alpha_1 \alpha_2 + \alpha_+ \alpha_-, \quad (66b)$$

$$\mathcal{D}_{13}^{(-)} = \mathcal{D}_{31}^{(-)} = \alpha_1 \alpha_+, \mathcal{D}_{14}^{(-)} = \mathcal{D}_{41}^{(-)} = \alpha_1 \alpha_-, \quad (66c)$$

$$\mathcal{D}_{23}^{(-)} = \mathcal{D}_{32}^{(-)} = \alpha_2 \alpha_+, \mathcal{D}_{24}^{(-)} = \mathcal{D}_{42}^{(-)} = \alpha_2 \alpha_-, \quad (66d)$$

$$\mathcal{D}_{34}^{(-)} = \mathcal{D}_{43}^{(-)} = \alpha_1 \alpha_2 + \alpha_+ \alpha_-, \quad (66e)$$

and $\mathcal{D}^{(+)}$ as $\mathcal{D}^{(-)}$ after swapping α_k and α_k^+ .

REFERENCES

- [1] R. Loudon and P. L. Knight, ‘‘Squeezed light’’, *J. Mod. Opt.* **34**, 709 (1987).
- [2] D. F. Walls and G. J. Milburn, *Quantum Optics* (Springer, Berlin, 1994).
- [3] P. D. Drummond and Z. Ficek (eds.), *Quantum Squeezing* (Springer, Berlin, 2004).
- [4] S. L. Braunstein and P. van Loock, ‘‘Quantum information with continuous variables’’, *Rev. Mod. Phys.* **77**, 513 (2005).
- [5] H. Vahlbruch, M. Mehmet, S. Chelkowski, B. Hage, A. Franzen, N. Lastzka, S. Goßler, K. Danzmann, and R. Schnabel, ‘‘Observation of Squeezed Light with 10-dB Quantum-Noise Reduction’’, *Phys. Rev. Lett.* **100**, 033602 (2008).
- [6] Y. Takeno, M. Yukawa, H. Yonezawa, and A. Furusawa, ‘‘Observation of -9 dB quadrature squeezing with improvement of phase stability in homodyne measurement’’, *Opt. Express* **15**, 4321 (2007)
- [7] C. Navarrete-Benlloch, E. Roldán, and G.J. de Valcárcel, ‘‘Noncritically Squeezed Light via Spontaneous Rotational Symmetry Breaking’’, *Phys. Rev. Lett.* **100**, 203601 (2008).
- [8] C. Navarrete-Benlloch, A. Romanelli, E. Roldán, and G.J. de Valcárcel, ‘‘Non-critical squeezing in 2-transverse-mode optical parametric oscillators’’, arXiv: 0904.0049 (2009).
- [9] C. Navarrete-Benlloch, G.J. de Valcárcel, and E. Roldán, ‘‘Generating highly squeezed Hybrid Laguerre–Gauss modes in large Fresnel number Degenerate Optical Parametric Oscillators’’, accepted in *Phys. Rev. A* (2009).
- [10] N. Hodgson and H. Weber, *Laser resonators and beam propagation* (Springer, New York, 2005).
- [11] P.D. Drummond and C.W. Gardiner, ‘‘Generalised P-representations in quantum optics’’, *J. Phys. A: Math. Gen.* **13**, 2353 (1980).
- [12] H.J. Carmichael, *Statistical Methods in Quantum Optics I* (Springer, Berlin, 1999).
- [13] C. W. Gardiner and P. Zoller, *Quantum Noise* (Springer, Berlin, 2000).
- [14] I. Pérez-Arjona, E. Roldán, and G.J. de Valcárcel, ‘‘Quantum squeezing of optical dissipative structures’’, *Europhys. Lett.* **74**, 247 (2006)
- [15] I. Pérez-Arjona, E. Roldán, and G.J. de Valcárcel, ‘‘Theory of quantum fluctuations of optical dissipative structures and its application to the squeezing properties of bright cavity solitons’’, *Phys. Rev. A* **75**, 063802 (2006).
- [16] J. Gea-Banacloche, N. Lu, L.M. Pedrotti, S. Prasad, M.O. Scully, and K. Wódkiewicz, ‘‘Treatment of the spectrum of squeezing based on the modes of the universe. I. Theory and a physical picture’’, *Phys. Rev. A* **41**, 369 (1990).